American Mineralogist, Volume 68, pages 634–641, 1983

Bannermanite, a new sodium-potassium vanadate isostructural with β-$Na_xV_6O_{15}$

JOHN M. HUGHES[1]

Department of Earth Sciences, Dartmouth College, Hanover, New Hampshire 03755

AND LARRY W. FINGER

Geophysical Laboratory, Carnegie Institution of Washington, Washington, D. C. 20008

Abstract

Bannermanite, $(Na,K)_xV_x^{4+}V_{6-x}^{5+}O_{15}$ ($0.90 > \times > 0.54$), a natural vanadium oxide bronze compound, occurs as black subhedral to euhedral crystals in the oxide zone of a fumarole at Izalco volcano, El Salvador, Central America. The mineral is associated with shcherbinaite, stoiberite, and ziesite. Bannermanite is monoclinic, space group $C2/m$, with a = 15.413(7), b = 3.615(2), c = 10.066(8)Å, β = 109.29(8)°, Z = 2, D(obs) = 3.5±0.2 g/cm^3, and D(calc) = 3.55 g/cm^3. The crystal structure of bannermanite has been refined to wR = 0.074 from the vanadium oxide bronze structure model. The structure consists of a clinolattice of VO_5 square-based pyramids and VO_6 octahedra. This array of V–O polyhedra forms rectangular tunnels in which Na and K ions occur. The vanadium ions are in two charge states, V^{4+} and V^{5+}, with the number of vanadium ions in the reduced state equal to the number of alkali ions in the tunnel sites; thus, charge balance is maintained.

Bannermanite transmits light on thin edges, with a mean index of refraction of 2.2, on the basis of the rule of Gladstone and Dale. The mineral has two cleavages, ($h0l$) and ($0kl$), and a dark gray-black streak. It is named in honor of the late Dr. Harold M. Bannerman.

Introduction

Naturally occurring $(Na,K)_xV_x^{4+}V_{6-x}^{5+}O_{15}$ has been discovered in the fumaroles in the summit crater of Izalco volcano, El Salvador, Central America (13°49′N; 89°38′W). Identification of this mineral as the potassium-bearing analog of NaV_6O_{15} is based on electron probe microanalysis and X-ray diffraction analysis. The new mineral is named bannermanite in honor of the late Dr. Harold M. Bannerman. Dr. Bannerman had a long and distinguished career in the field of geology and served in such posts as Chief of the Non-metalliferous Geology Section of the U.S. Geological Survey, Chief of the Division of Economic Geology of the U.S.G.S., and Professor of Geology, Dartmouth College. The type specimen of bannermanite is currently on deposit at the Department of Earth Sciences, Dartmouth College. Cotype specimens are on deposit at the Smithsonian Institution and the Geological Museum of Harvard University. The total amount of the mineral is a few milligrams. The mineral and mineral name have been approved by the Commission on New Minerals and Mineral Names of the International Mineralogical Association.

Locality and occurrence

Izalco volcano is a basaltic composite cone that has been intermittently active since its birth in 1770. The volcano rises to an altitude of 1965 m, with 650 m relief, and has an approximate volume of 2 km^3. The geology of the volcano is described by Meyer-Abich (1958), Rose and Stoiber (1969), and Stoiber *et al.* (1975).

Since 1963 the fumarolic gases and sublimate minerals of the summit crater have been extensively studied (Stoiber and Durr, 1963; Stoiber and Rose, 1970, 1974; Stoiber *et al.*, 1975; Birnie and Hughes, 1979; Hughes and Birnie, 1980b). Vanadium was found to be a distinctive element in the minerals of the sublimate suite, which includes such vanadium minerals as shcherbinaite ($V_6^{5+}O_{15}$), stoiberite ($Cu_5^{2+}V_2^{5+}O_{10}$), and ziesite (β-$Cu_2^{2+}V_2^{5+}O_7$.

Bannermanite is found in the MR and L fumaroles (Stoiber *et al.*, 1975) at Izalco volcano as a black incrustation coating basaltic breccia fragments. The mineral occurs as subhedral to euhedral crystals up to approximately 250 μm in greatest dimension. It is intimately associated with shcherbinaite.

Introduction to oxide bronzes

The oxide bronzes are compounds of the class M_xTO_n, where M is an electropositive metal ion such as Na or K,

[1] Present address: Department of Geology, Miami University, Oxford, Ohio 45056.

0003–004X/83/0506–0634$02.00

and T is a transition metal ion such as vanadium. In this class of compounds, the metal ion M is located in a covalent network of T–O ions. The M ions donate electrons to the covalent subarray that are either localized at certain T sites, producing a semiconducting phase, or delocalized within the TO_n subarray, producing a metallic phase. Hagenmuller (1973) has summarized data on the oxide bronzes on which much of the following section is based.

Because of the variable oxidation states of the T ions, the value of x can vary over a range greater than most nonstoichiometric binary compounds (*e.g.*, pyrrhotite). Generally, the mean oxidation state $(2n - x)$ lies between the highest oxidation value of the transition element (p) and the value $(p - 1)$.

Oxide bronze phases occur with several transition metals. Oxide bronzes of tungsten have long been known, and more recently vanadium oxide bronzes have been investigated. Similar compounds of molybdenum, niobium, and tantalum have also been synthesized.

The vanadium oxide bronzes, unlike the bronzes of other transition metals, form a wide variety of structures. This variety is due to the relatively small size and range in ionic-covalent nature of the vanadium ion as compared to other oxide bronze forming transition metals. Whereas the larger transition metal ions form a regular covalent network of T–O octahedra, the vanadium octahedra are often distorted, even to the point of forming five-coordinated square-based pyramids. This distortion results in complex vanadium bronze structure types and imparts a strong anisotropy to some of their physical properties.

Synthetic $Na_xV_x^{4+}V_{6-x}^{5+}O_{15}$ was initially synthesized and investigated by Flood and Sorum (1943), who found the limits of composition to be $0.45 \leq x \leq 0.93$. In a perceptive study of particular interest to the present work, Wadsley (1955) found the upper limit of Na concentration extended to $x = 0.99$. He solved the structure of a crystal with maximum Na, thus defining the oxide bronze structure type and providing the structural explanation for the nonstoichiometric nature of the compound.

Several studies of other oxide bronze structure types have been undertaken since Wadsley's work. These studies have confirmed his conclusions and elucidated the crystal chemistry of the oxide bronzes. In the $M_xV_2O_5$ system several ranges of concentration of the alkali ion M have been defined and several other types of vanadium oxide bronze structures have been isolated. These alkali ion concentration ranges vary with the particular ion. The compositional ranges for M = Na are particularly germane to the present study and are summarized in Figure 1.

The sodium-poor region of the solid solution depicted in Figure 1 is of interest because of two minerals with these compositions. The α-phase ranges from pure shcherbinaite ($V_6^{5+}O_{15}$) to $Na_{0.06}V_{0.06}^{4+}V_{5.94}^{5+}O_{15}$ at 600°C (Hagenmuller, 1973). These compositions are limiting

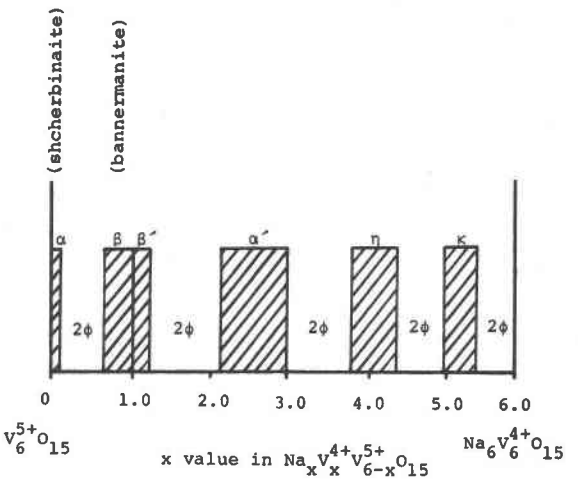

Fig. 1. Range of isotypic solid solutions in oxide bronze system $Na_xV_x^{4+}V_{6-x}^{5+}O_{15}$. Striped areas represent single-phase regions, with phase designation above regions. Phase regions determined for synthetic phase at 600°C (Hagenmuller, 1973).

phases in an isostructural series based on the V_2O_5 structure (Hagenmuller, 1973; Hughes and Finger, in preparation). With increasing Na concentration, the orthorhombic V_2O_5 structure becomes unstable and the monoclinic β-phase (bannermanite) is formed with compositional limits of $0.66 < x < 1.0$ for $Na_xV_x^{4+}V_{6-x}^{5+}O_{15}$ at 600°C (Hagenmuller, 1973). For $1.0 < x < 1.2$, the β' phase, which is structurally similar to bannermanite, is stable; however, the Na in excess of $x = 1.0$ fills sites that are not occupied in bannermanite (Hagenmuller, 1973).

Chemical composition

A chemical analysis of the type specimen of bannermanite is given in Table 1. The analysis was obtained with a three-spectrometer JEOL-35C electron probe microanalyzer and vanadium metal (V), orthoclase (K), and diopside–jadeite (Na) as standards. Because of the thinness of the crystals, the accelerating voltage was reduced to 10 kV; beam current on the flag was 207 pA. A complete energy-dispersive analysis was run, and no elements with $Z > 11$, other than K, Na, and V, were detected above background.

An average of 58 analyses of 15 crystals gave the formula $(Na_{0.6}K_{0.1})$ $(V_{0.7}^{4+}V_{5.3}^{5+})O_{15}$ on the basis of O = 15. The alkali site occupancy ranged from 0.54 to 0.90 with a mean of 0.70 and a standard deviation of 0.07. The average Na/K molar ratio was 6.0. X-ray images of bannermanite taken on (001) showed no zonation of Na and K within the crystals.

Because bannermanite occurs intimately intergrown with shcherbinaite, it appears that these minerals coexist in the two-phase field including the most Na-rich shcherbinaite and most Na-deficient bannermanite (Fig. 1).

Table 1. Electron microprobe analyses of bannermanite (wt.%).

	1	2	Atoms (O=15)
Na_2O	3.03(9)*	3.03	0.56
K_2O	1.26(8)	1.26	0.15
V_2O_4	...	10.36	0.71
V_2O_5	95.98(63)	84.62	5.29
	100.27	99.27	

*One standard deviation of least units cited in parentheses.

1. Mean of six analyses of holotype crystal with all V calculated as V_2O_5.

2. Recalculated analyses with V_2O_4 required for charge balance.

Formula of type specimen on the basis of O = 15: $(Na_{0.56}K_{0.15})V^{4+}_{0.71}V^{5+}_{5.29}O_{15}$.

X-ray crystallography

Bannermanite was first identified by comparison of its diffraction pattern with that of NaV_6O_{15} (JCPDS #24-1155). The bannermanite pattern was obtained with a 114.6 mm Gandolfi camera and Cr$K\alpha$ radiation (2.2909Å, V filter) in a helium atmosphere. Intensities were visually estimated. Observed and calculated diffraction patterns have been contributed to the JCPDS file.

Single-crystal a- and c-axis precession photographs were taken with Mo$K\alpha_1$ radiation (0.70930Å, Zr filter). The results of the precession study showed bannermanite to be monoclinic with space group Cm, $C2$, or $C2/m$. Space group $C2/m$ was chosen on the basis of the work of Wadsley (1955) and Ozerov (1957), both of whom demonstrated a center of symmetry in the compound. Reflections were limited by the condition $h + k = 2n$.

The unit-cell parameters of bannermanite were refined by a least-squares method with angles from nine reflections measured on an automated four-circle diffractometer. These cell parameters are listed in Table 2 along with those of the synthetic isostructural compounds reported by Wadsley (1955), Ozerov (1957), and Erdos (JCPDS 24-1155 and personal communication). Erdos reported the space group as $A2/m$, but the a and c axes of bannermanite have been reversed to conform to the convention of $a > c$ in monoclinic crystals. The beta angle determined by Erdos was erroneously reported on JCPDS 24-1155 as 109.45°, and the correct value of 109.27° is given in table 2 (Erdos, pers. comm.).

Crystal structure

Hundreds of crystals were examined optically, and 15 precession suites were obtained in order to find a single crystal large enough for a structure refinement. The crystal selected is a rectangular parallelepiped, 11 × 46 × 101 μm in size. Precession ($hk0$) and ($0kl$) photographs of this crystal showed no evidence of twinning or polycrystalline intergrowths.

Integrated intensity data were collected with an automated Picker four-circle diffractometer. All reflections within the hemisphere of reciprocal space encompassing $\pm h$, $+k$, and $\pm l$ within the 2θ range of 0–60° were collected with the $\theta/2\theta$ scan mode and Nb-filtered Mo$K\alpha_1$ radiation (0.70930Å). Peaks were scanned at 1/2° per min for 4 min over the peak. Stationary backgrounds were taken for 2 min at each end of the peak scan. To standardize, the 020 and 006 reflections were measured every 4 hours. The resulting intensity data were corrected for Lorentz and polarization effects. A numerical integration technique (Burnham, 1966) was used to correct for absorption. The effectiveness of this correction was verified with a 360° psi scan at 5° intervals on the 200 reflection. This reflection would exhibit the greatest variation in transmission intensity. The linear absorption coefficient (μ) for bannermanite is 51.0 cm^{-1}.

Structure factors of symmetry equivalent reflections were then averaged. A reflection was considered observed if the average structure factor was greater than

Table 2. Unit cell parameters of natural and synthetic bannermanite

	a(A)	b(A)	c(A)	β(deg.)	Reference
$Na_{0.99}V_6O_{15}$	15.44	3.61	10.08	109.6	Wadsley (1955)
NaV_6O_{15}	15.335	3.605	10.039	109.2	Ozerov (1957)
NaV_6O_{15}	15.38	3.61	10.07	109.27	Erdos* (JCPDS 24-1155)
Bannermanite	15.413(7)**	3.615(2)	10.066(8)	109.29(8)	This study

*Erroneous value of β (109.45°) corrected (Erdos, personal communication).

**esd's of least units cited in parentheses.

Values of a and c axes reversed to conform with convention of a>c in monoclinic crystals.

Table 4. Atomic coordinates and anisotropic thermal parameters for bannermanite

Atom	x	y	z	B equiv.	β_{11}	β_{22}	β_{33}	β_{13}
V(1)	0.3370(2)	0	0.1030(3)	0.75(4)	0.0011(1)	0.009(2)	0.0029(2)	0.0012(1)
V(2)	0.1163(2)	0	0.1176(2)	0.54(4)	0.0008(1)	0.007(2)	0.0020(2)	0.0008(1)
V(3)	0.2873(2)	0	0.4100(2)	0.84(5)	0.0013(1)	0.014(2)	0.0024(3)	0.0010(1)
O(1)	0	0	0	1.2(2)	0.0020(7)	0.007(11)	0.004(2)	0.0006(8)
O(2)	0.8171(7)	0	0.058(1)	0.8(2)	0.0017(5)	0.004(7)	0.003(1)	0.0017(6)
O(3)	0.6342(7)	0	0.078(1)	0.9(2)	0.0014(5)	0.012(8)	0.004(1)	0.0022(6)
O(4)	0.4354(8)	0	0.218(1)	1.6(2)	0.0021(5)	0.03(1)	0.003(1)	0.0006(6)
O(5)	0.2618(7)	0	0.221(1)	1.3(2)	0.0017(5)	0.04(1)	0.002(1)	0.0012(6)
O(6)	0.1070(7)	0	0.272(1)	1.1(2)	0.0014(5)	0.020(9)	0.005(1)	0.0019(6)
O(7)	0.7554(8)	0	0.426(1)	1.2(2)	0.0037(6)	0.002(7)	0.003(1)	0.0027(7)
O(8)	0.3952(8)	0	0.469(1)	2.1(2)	0.0020(6)	0.06(1)	0.004(1)	0.0012(7)
Na	0.002(1)	0	0.411(2)	1.9(5)	0.0017(9)	0.04(2)	0.006(2)	0.001(1)

$\beta_{12} = \beta_{23} = 0$ for all atoms.

1.414 times the standard deviation of the average structure factor, corresponding to 2 times the standard deviation of the intensity. Of the 848 structure factors measured, only 679 were thus considered observed. The observed and calculated structure factors are listed in Table 3.[2]

The structure was refined by a full-matrix, least-squares method (RFINE4, Finger and Prince, 1975) with a weighting scheme based on counting statistics. Neutral atom scattering curves from Cromer and Mann (1968) were used, with corrections for anomalous dispersion.

The atomic positions for NaV_6O_{15} (Wadsley, 1955) were used to initiate the refinement. Individual atom isotropic temperature factors (V = 0.60, O = 0.80, Na = 1.30) were assigned. Total Na occupancy was initially set at $Na_{0.40}V_6O_{15}$, slightly below the limit observed in bannermanite. The initial cycles included refinements of scale factor, atomic positions, isotropic temperature factors, Na occupancy, and extinction factor. This last parameter did not deviate significantly from zero; thus it was excluded from later refinement cycles. After four cycles the refinement converged at $wR = 0.090$. All atom positions were then refined with anisotropic temperature factors. After cycle 9 the structure converged at $wR = 0.074$, and $R = 0.094$ for all observed reflections. The structure model probably did not refine below this level because of the small crystal size and concommitant lower level of counting precision. The atomic coordinates and anisotropic temperature factors for bannermanite are given in Table 4.

The alkali site [4(*i*)] can be occupied by Na, K, or a vacancy. The electron occupancy of the alkali site was determined by refining total electron occupancy of the site with Na scattering curves. After nine cycles of refinement the model placed 1.52 Na atoms in the unit cell or 0.76 atom in the asymmetric unit. Independent microprobe data showed, however, that this site is occupied by Na and K in an average molar ratio of 6:1. When the total number of electrons associated with 0.76 Na atom is distributed between Na and K in a ratio of 6:1, this site occupancy becomes $Na_{0.6}K_{0.1}$.

Wadsley's (1955) structure model for NaV_6O_{15} is equivalent to the bannermanite model within the relatively large error limits of his early determination. The greatest discrepancy occurs in the alkali site coordinates. Ozerov (1957) also noted a discrepancy between alkali site coordinates in KV_6O_{15} and Wadsley's NaV_6O_{15}.

All atoms except O(1) are located in the special 4(*i*) position; O(1), located at the origin, is in the special 2(*a*) position. All atoms in 4(*i*) and 2(*a*) are constrained to lie on plans at $y = 0$ or $y = ½$, a consequence of the short 3.6Å *b* dimension in bannermanite, a length common in other oxyvanadates.

Hagenmuller (1973) describes the oxide bronze structures as ones in which an electropositive metal ion (M) is contained in a covalent transition metal (T) and oxygen array. The T–O array in bannermanite consists of distorted VO_6 octahedra that form zig-zag sheets perpendicular to c^* (Figs. 2, 3). These V(1)–O_6 and V(2)–O_6 octahedral pairs are linked to adjacent octahedral pairs with the same *y* value through corner sharing of O(1); adjacent octahedral pairs along *b* are linked through edge sharing. The sheets of octahedra are linked by two V(3)–O_5 square-based pyramids that are joined by edge sharing, and are linked to the zig-zag octahedral sheets by corner sharing through O(5), the oxygen atom shared by V(1), V(2), and V(3). Ozerov (1957) has shown how this T–O array is derived from the structure of V_2O_5 by a distortion of the orthogonal lattice of the V_2O_5 structure to form the monoclinic lattice of bannermanite (Fig. 3). This distortion accommodates the monovalent alkali ions in the oxide bronze phase.

The covalent nature of the vanadium ion leads to VO_6

[2] To receive a copy of Table 3, order Document AM-83-217 from the Business Office, Mineralogical Society of America, 2000 Florida Avenue, N.W., Washington, D. C. 20009. Please remit $1.00 in advance for the microfiche.

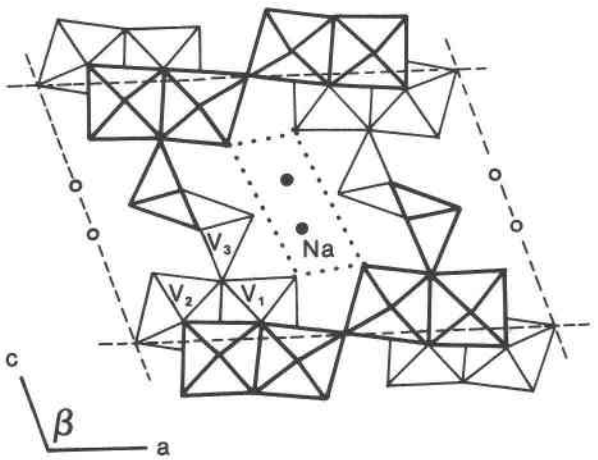

Fig. 2. Polyhedral projection on (010) of bannermanite. Bold lines outline polyhedra centered at $y = ½$; lighter lines outline polyhedra centered at $y = 0$. Na ligands are omitted. Dotted lines outline projection of tunnels in structure (after Hagenmuller, 1973).

octahedra that are typically highly distorted (Goodenough, 1970), for example V(1)–O_6 and V(2)–O_6 in bannermanite. The mean V–O bond length for V(1) is 1.937Å, with a range of 1.575–2.391Å, and that for V(2) is 1.939Å, with a range of 1.607–2.315Å (Table 5). The square-based pyramid V(3)–O_5 has an extreme degree of "octahedral" distortion. One of the four oxygen atoms, O(6), normally coplanar in (010) with vanadium in the VO_6 octahedron, is so far removed from V(3) (2.67Å) that it is not considered to be involved in the coordination polyhedron. The remaining five oxygen atoms coordinate V(3) in a square-based pyramid with an average bond length of 1.827Å. The O(6) atom coordinates the monovalent alkali ion in the 4(*i*) site in bannermanite.

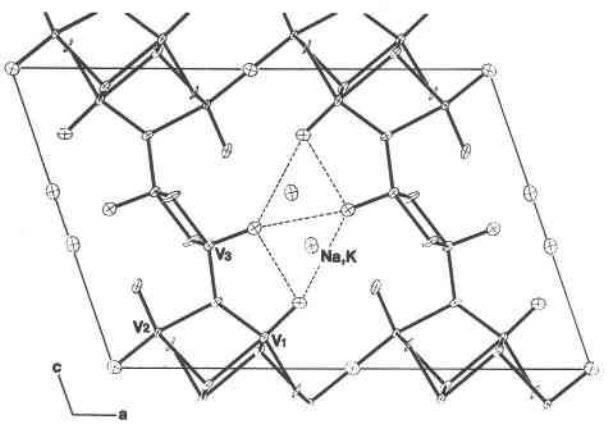

Fig. 3. ORTEP (Johnson, 1965) plot of bannermanite structure projected on (010) with 50% probability ellipsoids. Dashed lines indicate the projections of the trigonal prisms that coordinate alkali atoms. All atoms lie on mirror planes at $y = 0$ or $y = ½$.

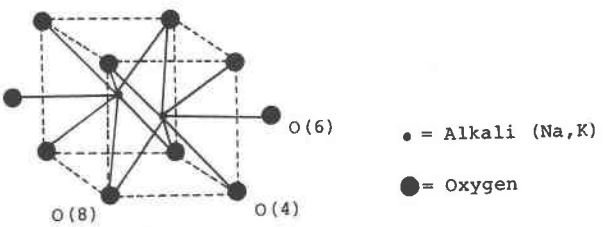

Fig. 4. Coordination polyhedron of alkali ions in bannermanite. The nonorthogonal parallelepiped outlined by dashed lines has 2/*m* symmetry, with the vertical two-fold axis parallel to *b* and located between the alkali metal sites, each of which has a maximum occupancy of 0.5. The mirror plane contains the alkalies and the O(6) atoms (after Darriet, 1971).

The alkali (Na,K) sites are coordinated by seven oxygen atoms (Fig. 4). The Na atoms lie in tunnels parallel to *b*. The nearly rectangular tunnels are formed by O(4) and O(8) at $y = 0$ and 1, and O(6) at $y = ½$. Within these tunnels, the seven-coordinated alkali ions are bonded to six oxygens at the corners of a distorted trigonal prism; whereas the seventh bond is to an oxygen lying on a prism face. The (Na,K)–O bond lengths vary from 2.43 to 2.64Å, with a mean of 2.55Å. This coordination of sodium by seven oxygen atoms is rare, but not unknown; six other minerals (darapskite, glauberite, krohnkite, narsarsukite, ramsayite, and vanthoffite) have this type of coordination, with a mean bond length of 2.51Å. The bannermanite polyhedron is the most regular of these seven examples, with bond lengths that differ by only 0.21Å.

The multiplicity of the alkali ion site is 4; therefore, if all alkali sites were occupied, the formula corresponding to the asymmetric unit would be $Na_2V_6O_{15}$. It has been established that the upper limit of alkali concentration of the beta oxide bronze phase (bannermanite) is $Na_1V_6O_{15}$; thus, the alkali sites are never more than ½ occupied (Hagenmuller, 1973). In natural bannermanite the composition range has been found to extend from $(Na,K)_{0.54}V_6O_{15}$ to $(Na,K)_{0.90}V_6O_{15}$, with an average alkali site occupancy of $Na_{0.6}K_{0.1}V_6O_{15}$. This range of values is within that reported for the synthetic Na phase by Wadsley (1955).

Table 5. Selected bond lengths in bannermanite

Bond	Distance (A)	Bond	Distance (A)
V(1)-O(2)	1.865(3)	V(3)-O(5)	1.808(9)
-O(2)	1.865(3)	-O(7)	1.894(3)
-O(2)	2.39(1)	-O(7)	1.894(3)
-O(3)	2.013(9)	-O(7)	1.967(9)
-O(4)	1.58(1)	-O(8)	1.57(1)
-O(5)	1.916(9)	-O(6)	2.67(1)
Mean of 6	1.937	Mean of 5	1.827
V(2)-O(1)	1.792(3)	Na-O(4)	2.61(1)
-O(2)	2.315(9)	-O(4)	2.61(1)
-O(3)	1.890(3)	-O(6)	2.46(2)
-O(3)	1.890(3)	-O(8)	2.44(1)
-O(5)	2.14(1)	-O(8)	2.44(2)
-O(6)	1.607(9)	-O(8)	2.64(2)
		-O(8)	2.64(2)
Mean of 6	1.939	Mean of 7	2.55

The possible occupancy arrangements of the alkali sites for theoretical $Na_2V_2^{4+}V_4^{5+}O_{15}$ are shown in Figure 5a, where all possible 4(*i*) alkali sites are filled. In this arrangement, however, the two adjacent alkali ions coplanar in (010) are separated by only 1.81Å. This distance is unreasonably close for two large positive ions; thus, these sites are never more than ½ occupied. The half-occupancy results in the end-member phase $NaV^{4+}V_5^{5+}O_{15}$ (Fig. 5b). Because the structure is centrosymmetric (Wadsley, 1955) with no superstructure, the vacancy-alkali ordering must be random. Thus, although any individual alkali chain must have the ordered configuration of NaV_6O_{15}, these chains would be randomly translated by 0 or 1 *b* in the adjacent chain, retaining the statistical 2/*m* symmetry of the cell. Each chain is ordered with respect to alkali ion distribution, but the chains themselves must be disordered with respect to each other.

As the alkali occupancy falls to less than 50% of the total sites ($Na_xV_x^{4+}V_{6-x}^{5+}O_{15}$, $x < 1$), the ions are randomly removed from the alkali chains (Fig. 5c). Crystals of bannermanite with $x \sim 0.7$ retain 2/*m* diffraction symmetry; therefore, alkali vacancies must be random. In the single crystal used in this structure study, the compositional refinement converged at a composition of $Na_{0.59}K_{0.10}V_6O_{15}$, the average value observed for other bannermanite crystals. Thus, 1.4 of the 4 alkali sites are occupied.

The existence of monovalent ions in the V-O subarray necessitates a charge reduction that is accommodated by the reduction of one V^{5+} to V^{4+} for each monovalent insertion ion. Hagenmuller (1973) suggested that these V^{4+} centers are located in the zig-zag VO_6 sheets, because V^{5+} ions have a strong affinity for the square-based pyramidal coordination in the structure. In bannermanite the transition metal valence is controlled by the presence of an electron donor (Na) and not by the fugacity of oxygen, an electron receptor. With greater Na concentration within the phase, the mean oxidation state of the V is lowered (Dickens *et al.*, 1973).

Numerous studies of the electronic properties of the beta vanadium oxide bronze phase have been undertaken in order to determine the manner of charge balance within these crystals. These studies are best summarized in the report of Perlstein and Sienko (1968). They found that the conduction band model of electron transport could not describe their measurements, which could be explained, however, by the concept of a small polaron. In the simplest form of this model, the electron is considered to be self-trapped at a local site because of induced distortions of the surrounding ions. At moderate to high temperatures the electron can become delocalized and can jump from site to site. In sodium vanadium bronze the V(1)–V(2) spacing is only slightly greater than the critical value for electron delocalization in the octahedral sheets. Measurements of the Seebeck effect, Hall voltage, electrical conductivity, and magnetic susceptibility of the phase indicate that the V^{4+} centers are statistically localized in the octahedral sheet and jump parallel to *b* between centers in this sheet. This small-polaron model accounts for the remarkable anisotropic conductivity in the beta oxide bronze phase, with the conductivity along *b* more than 600 times greater than that perpendicular to *b* (Ozerov, 1957). In a more recent study of the electron structure of the phase, Cherkashenko *et al.* (1980) examined the electron delocalization mechanism by measuring the orientation dependence of two low-energy vanadium X-ray emission spectra. Their results could also be explained by electron delocalization along the *b* axis in the V_1 and V_2 octahedral sheet. Furthermore, they found that the electron jumps occur not by direct V–V interactions, but through the intermediate oxygen atoms O_2 and O_3 (Fig. 3) for V_1–V_1 and V_2–V_2 jumps, respectively.

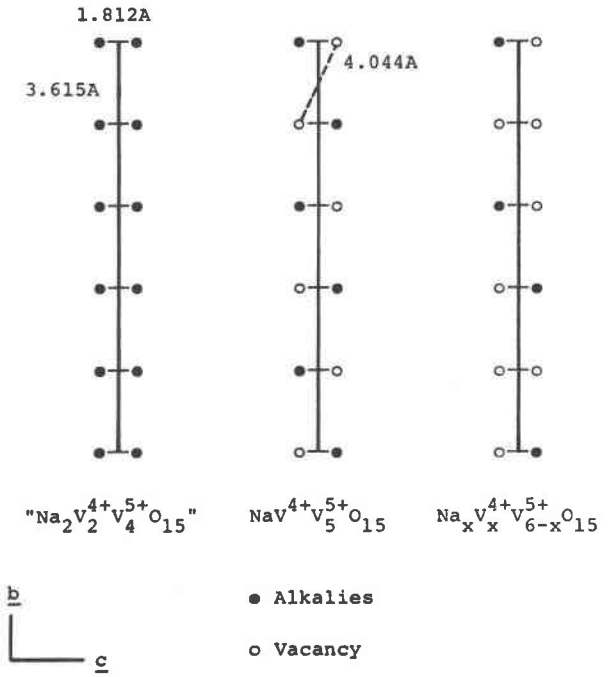

Fig. 5. Possible alkali ion locations in oxide bronze phases.

Nature of solid solution

Bannermanite displays a wide range of isostructural compositional variation. The solid solution can be classified as the hollandite type or nonstoichiometric stuffed type. In this type of compound nonneutral units (Na^+) are present in the structure in amounts that can vary over a wide compositional range; charge balance within the structure is maintained by the existence of two oxidation states of transition metal ions within the phase. As noted by Wadsley (1955, p. 695) in his definition of this solid solution type, bannermanite is a compound in which "a host (V_2O_5), crystallizing in the presence of ions incapable of substitution, may form a new phase embodying tubes or tunnels which afford the foreign ions (Na,K) a

normal environment and will not necessarily require integral numbers in a unit formula."

Physical properties

Bannermanite occurs as black, submetallic, subhedral to euhedral, lath-like crystals flattened on (001) and elongated up to 250 μm along b. The aspect ratio (length/width) of the laths varies from approximately 2 to 50.

Because of the morphology and crystal size of bannermanite, optical observations were made only with (001) parallel to the microscope stage. Along thin edges, bannermanite is light brown in transmitted light (color similar to 5YR 5/6; Goddard *et al.*, 1963). Moderate absorption is observed, $b > a$. The crystals were observed to be length slow; thus b coincides with beta or gamma. The mean index of refraction, calculated by the rule of Gladstone and Dale, is 2.2 as calculated from specific refractivity values from Jaffee (1956) for V_2O_5 and Larsen and Berman (1934) for Na_2O and K_2O.

The streak of bannermanite is dark gray-black (similar to N2.5, Goddard *et al.*, 1963). Bannermanite is brittle, and it does not fluoresce in short- or long-wave ultraviolet radiation.

The density calculated from the X-ray unit-cell volume and the average chemical formula is 3.55 g/cm^3. The magnetic fluid method (Hughes and Birnie, 1980a) gave a measured density of 3.5±0.2; thus, Z = 2.

Because of the morphology and crystal size of bannermanite, observations of cleavages are limited to the trace of their intersection with (001). In this orientation many grains show a perfect ($h0l$) and a fair ($0kl$) cleavage, assumed to be (100) and (010), respectively.

The structural cause for the perfect (100) cleavage can be seen in Figures 2 and 3. As noted previously, the V(1) and V(2) octahedra in the zig-zag octahedral sheets are joined by edge sharing along b and by corner sharing along a. The breaking of the single V(2)–O(1)–V(2) bond accounts for the perfect cleavage perpendicular at a^*. This orientation also obviates the need to cleave bonds through the V(3)–O_5 square-based pyramids; according to the electrostatic valence principle, these are the stronger of the V–O bonds in the structure because of their lower coordination number. Any cleavage other than (100) would necessitate cleaving these bonds.

The thermal properties of $NaV^{4+}V^{5+}{}_5O_{12}$ were studied by Ozerov (1957). His examination of the thermal curves showed two sharp endothermic effects, one at 590° and one at 738°; he attributed the effect at 738°C to fusion. The cooling curves showed another effect at 652°C. Ozerov examined heated single crystals of the phase at 20°, 620°, and 700°C, and found no evidence in the film of structural changes other than thermal expansion. He concluded that the aberrations in the thermal curves are due to unobservable structural changes, such as a rearrangement of alkali ions in the partially occupied alkali metal sites.

The magnetic properties of $Na_{0.99}V_6O_{15}$ were studied by Schlenker *et al.* (1979) at low temperatures. They found a magnetic transformation at approximately 18 K and measured initial reversible susceptibility, thermoremanent and isothermal remanent magnetization for different crystallographic orientations at temperatures below the transition. The magnetic properties are similar to those of an antiferromagnet; however, the remanent magnetizations are inconsistent with this interpretation. They proposed disorder of V^{4+}, which is consistent with random placement of Na^+ and local charge balance, to explain their results. It also appears that there is weak ferromagnetism along the b-axis.

Acknowledgments

The crystal structure portion of this research was undertaken while Hughes was a Predoctoral Fellow at the Geophysical Laboratory of the Carnegie Institution of Washington. H. S. Yoder, Jr., Director, is gratefully acknowledged for that opportunity. The manuscript was greatly improved by reviews by, and discussions with, R. W. Birnie, H. R. Naslund, and R. E. Stoiber, Dartmouth College; R. M. Hazen, R. L. Ralph, and N. Z. Boctor, Geophysical Laboratory; and M. H. Hickman, Miami University. C. H. Nielsen of JEOL U.S.A., Inc., provided access to the electron microprobe used in analyses of the bannermanite specimens. This work was supported in part by National Science Foundation grant EAR79-19768.

References

Birnie, R. W. and Hughes, J. M. (1979) Stoiberite, $Cu_5V_2O_{10}$, a new copper vanadate from Izalco volcano, El Salvador, Central America. American Mineralogist, 64, 941–944.

Burnham, C. W. (1966) Computation of absorption correction and the significance of the end effect. American Mineralogist, 51, 159–167.

Cherkashenko, V. M., Freidman, S. P., Gubanov, V. A., Kurmaev, E. Z., Volkov, V. L., and Fotiev, A. A. (1980) Electronic structure and anisotropy of X-ray emission spectra of NaV_6O_{15} monocrystal. Journal of Solid State Chemistry, 32, 377–387.

Cromer, D. T. and Mann, J. D. (1968) X-ray scattering factors computed from numerical Hartree-Fock wave functions. Acta Crystallographica, A24, 321–324.

Darriet, J. (1971) Etude Cristallochimique de Nouveaux de Substitution des Bronzes Oxygenes de Vanadium. Ph.D. Thesis, University of Bordeaux.

Dickens, P. G., Jewess, M., Neild, D. J., and Rose, J. C. I. O. (1973) Thermochemistry of oxide bronzes. Part 1. Sodium vanadium bronzes $Na_xV_2O_5$ with x between 0.2 and 0.22. Journal of the Chemical Society of London, Dalton Transactions, 1973, 30–33.

Finger, L. W. and Prince, E. (1975) A system of Fortran IV computer programs for crystal structure computations. U.S. National Bureau of Standards Technical Note, 854.

Flood, H. and Sorum, H. (1943) Om vanadylvanadat, en ny type elektriske halvedere. Tiddskrift for Kjemi, Berguesen og Metallurgi, Oslo, 5, 55.

Goddard, E. N., Trask, P. D., Deford, R. K., Rove, O. N., Singewald, J. T., and Overbeck, R. M. (1963) Rock-Color Chart. Huyskes-Enschede, Netherlands.

Goodenough, J. B. (1970) Interpretation of $M_xV_2O_5$-beta and $M_xV_{2-y}T_yO_5$-beta phases. Journal of Solid State Chemistry, 1, 349–358.

Hagenmuller, P. (1973) Tungsten bronzes, vanadium bronzes and related compounds. In A. F. Trotman-Dickenson, Ed., Comprehensive Inorganic Chemistry, Vol. 4, p. 541–605. Pergamon Press, New York.

Hughes, J. M. and Birnie, R. W. (1980a) Density determination of microcrystals in magnetic fluids. American Mineralogist, 65, 396–400.

Hughes, J. M. and Birnie, R. W. (1980b) Ziesite, β-$Cu_2V_2O_7$, a new copper vanadate and fumarole temperature indicator. American Mineralogist, 65, 1146–1149.

Jaffee, H. W. (1956) Application of the rule of Gladstone and Dale to minerals. American Mineralogist, 41, 757–777.

Johnson, C. K. (1965) A FORTRAN thermal ellipsoid plot program for crystal structure illustrations. U.S. National Technical Information Service, ORNL–3794.

Larsen, E. S. and Berman, H. (1934) The microscopic determination of the non-opaque minerals. U.S. Geological Survey Bulletin, 848.

Meyer-Abich, H. (1958) Active volcanoes of Guatemala and El Salvador. In F. Mooser, H. Meyer-Abich, and A. R. McBirney, Eds., Catalogue of the Active Volcanoes of the World Including Solfataras, Part VI, Central America, p. 39–105. International Association of Volcanology, Rome, Italy.

Ozerov, R. P. (1957) Crystal chemistry of the oxygen vanadium bronzes. Soviet Physics (Crystallography), 2, 219–224.

Perlstein, J. H. and Sienko, M. J. (1968) Single crystal studies of electrical conductivity, Seeback effect and Hall voltage in sodium vanadium bronze and a crystal-field model of electron transport. Journal of Chemical Physics, 48, 174–181.

Rose, W. I. and Stoiber, R. E. (1969) The 1966 eruption of Izalco volcano, El Salvador. Journal of Geophysical Research, 74, 3119–3130.

Stoiber, R. E. and Durr, F. (1963) Vanadium in the sublimates, Izalco volcano, El Salvador. (abstr.) Geological Society of America Special Paper, 76, 159.

Schlenker, C., Buder, R., Nguyen, V. D., Dumas J., Friederich, A., Kaplan, D. and Sol, N. (1979) Magnetic susceptibility of $Na_xV_2O_5$-β. Journal of Applied Physics, 50, 1720–1722.

Stoiber, R. E. and Rose, W. I. (1970) Geochemistry of Central American volcanic gas condensates. Bulletin of the Geological Society of America, 81, 2891–2912.

Stoiber, R. E. and Rose, W. I. (1974) Fumarolic incrustations at active Central American volcanoes. Geochimica et Cosmochimica Acta, 38, 495–516.

Stoiber, R. E., Rose, W. I., Lange, I. M., and Birnie, R. W. (1975) The cooling of Izalco volcano (El Salvador) 1964–1974. Geologische Jahrbuch, 13, 193–205.

Wadsley, A. D. (1955) The crystal structure of $Na_{2-x}V_6O_{15}$. Acta Crystallographica, 8, 695–701.

Manuscript received, April 15, 1982;
accepted for publication, October 13, 1982.